Melanoblasts' Proper Location and Timed Differentiation Depend on Notch/RBP-J Signaling in Postnatal Hair Follicles

Geneviève Aubin-Houzelstein Aubin Houzelstein, Johanna Dijan-Zaouche, Florence Bernex, Stéphanie Gadin, Véronique Delmas, Lionel Larue, Jean-Jacques J.-J. Panthier

Melanoblasts' Proper Location and Timed Differentiation Depend on Notch/RBP-J Signaling in Postnatal Hair Follicles

Geneviève Aubin-Houzelstein[1,2], Johanna Djian-Zaouche[1,2], Florence Bernex[1], Stéphanie Gadin[1], Véronique Delmas[3], Lionel Larue[3] and Jean-Jacques Panthier[1,2]

The Notch/RBP-J pathway is involved in a variety of developmental processes and in tissue homeostasis. In the melanocyte lineage, it has been shown that Notch signaling acts through *Hes1* to maintain the melanocyte stem cell population in the hair follicle. This study was designed to determine whether Notch signaling is implicated in other steps of melanocyte-lineage postnatal development. For this purpose, we developed mice in which the *RBP-J* gene was conditionally ablated in the melanocyte lineage and used the *Dct-lacZ* reporter transgene to track melanocytes and their precursors in individual hair follicles. We determine that Notch/RBP-J-deficient melanoblasts are in reduced number within the hair follicle and gather within its lower permanent part. Moreover, our results show that Notch signaling is necessary to prevent differentiation of melanocyte stem cells and of melanoblasts before they reach the hair bulb. Finally, our data show that Notch signaling is involved in proper location of melanoblasts in the outer root sheath and of melanocytes in the hair matrix. These findings reveal previously unrecognized roles for Notch signaling in the melanocyte lineage.

Journal of Investigative Dermatology advance online publication, 8 May 2008; doi:10.1038/jid.2008.120

INTRODUCTION

In the mouse skin, most melanocytes are found in the hair follicles (HFs) (Slominski and Paus, 1993). During development, melanocyte precursor cells emerge from the neural crest, migrate, and proliferate in the mesenchyme, colonize first the epidermis, then the forming HFs. There, they segregate to form two subpopulations: terminally differentiated, pigmented melanocytes, found in the hair matrix, responsible for the coloring of the hair shaft; and melanocyte stem cells (MSCs), found in an expanded region of the outer root sheath (ORS), the bulge, which corresponds to the lower permanent part (LPP) of the HF (Nishimura *et al.*, 2002). Throughout postnatal life, hair growth occurs in cycles. A finite period of hair fiber production (anagen) is followed by a regression phase (catagen) and a resting period (telogen). Melanogenesis is strictly coupled to the anagen stage of the hair cycle. During the first anagen, hair-matrix melanocytes differentiate directly from the embryonic melanoblasts bypassing MSCs (Mak *et al.*, 2006). They die by apoptosis during catagen. During the following anagens, the melanocyte population is renewed after stimulation of the MSCs. MSCs give rise to a transit-amplifying cell population; these committed and undifferentiated transit-amplifying cells are called melanoblasts (MBs) in the rest of this paper. The MBs exit the bulge and migrate downwards along the ORS to populate the hair matrix (Botchkareva *et al.*, 2001; Nishimura *et al.*, 2002). In the bulge, MSCs express a few known melanocyte markers, namely the dopachrome tautomerase (DCT) protein and the paired box transcription factor 3 PAX3 (Nishimura *et al.*, 2002; Lang *et al.*, 2005); they are negative for the proliferation marker Ki67 (Botchkareva *et al.*, 2001; Osawa *et al.*, 2005), suggesting that they are quiescent. Stem cell-derived MBs in the ORS and pigment-producing melanocytes in the hair matrix express numerous additional markers, including the receptor tyrosine kinase KIT, the basic helix–loop–helix zipper (bHLH-Zip) microphthalmia-associated transcription factor (MITF), the high-mobility group transcription factor SOX10 and proteins involved in melanin biosynthesis (Botchkareva *et al.*, 2001; Lang *et al.*, 2005; Osawa *et al.*, 2005).

The Notch pathway has pleiotropic actions during normal development and tissue homeostasis, and its dysfunction contributes to many cancers (Bolos *et al.*, 2007; Hurlbut *et al.*, 2007; Roy *et al.*, 2007). The Notch pathway regulates the developmental selection made by individual cells

[1]*INRA, UMR955 Génétique Moléculaire et Cellulaire; Ecole Nationale Vétérinaire d'Alfort, Maisons-Alfort, France;* [2]*Institut Pasteur, Unité de Génétique Fonctionnelle de la Souris; CNRS, URA 2578, Département de Biologie du Développement; USC INRA, Paris, France and* [3]*CNRS, UMR146 Génétique du Développement des Mélanocytes; Institut Curie, Bât. 110, Orsay, France*

Correspondence: Dr Geneviève Aubin-Houzelstein and Dr Jean-Jacques Panthier, Unité de Génétique Fonctionnelle de la Souris, Institut Pasteur, 25 rue du Docteur Roux, Paris F-75724, France.
E-mails: ghouzelstein@vet-alfort.fr and panthier@pasteur.fr

Abbreviations: β-gal, β-galactosidase; DCT, dopachrome tautomerase; E, embryonic day; HB, hair bulb; HF, hair follicle; KO, knockout; LPP, lower permanent part; MB, melanoblast; MSC, melanocyte stem cell; ORS, outer root sheath; P, postanatal day; TYRP1, Tyrosine-Related Protein 1; UPP, upper permanent part; UTP, upper transitory part

Received 18 January 2008; revised 3 March 2008; accepted 19 March 2008

according to the state of the adjacent cells (Artavanis-Tsakonas *et al.*, 1995, 1999). It is also frequently involved in the maintenance of populations of undifferentiated committed progenitors (Yoon and Gaiano, 2005). In addition, Notch signals are necessary for proliferation, migration, and rescue from apoptosis in various cell systems (Chiba, 2006). In mouse, four Notch genes (*Notch1* through *Notch4*) and five Notch ligands encoding genes (*Delta-like1, Delta-like3, Delta-like4, Jagged1*, and *Jagged2*) have been identified. As Notch receptors and their ligands are transmembrane proteins, Notch signaling requires direct cell–cell contact. On ligand binding, the Notch receptor is proteolytically cleaved, releasing its intracellular domain, NotchIC, from the membrane. NotchIC is then translocated to the nucleus, where it interacts with the recombination signal binding protein-J (RBP-J) within a multiproteic complex. The complex activates various target genes, such as members of the hairy and enhancer of split protein family. Importantly, all four mouse Notch-family members interact physically with RBP-J (Kato *et al.*, 1996).

In the melanocyte lineage, Notch signaling acts through *Hes1 (hairy/enhancer of split 1)* and plays a role in the maintenance of MSCs and MBs (Moriyama *et al.*, 2006; Pinnix and Herlyn, 2007; Schouwey *et al.*, 2007; Kumano *et al.*, 2008). Conditional ablation of *Rbp-J* in the melanocyte lineage produces a diluted coat color at birth and accelerates hair graying after the first hair moult (Moriyama *et al.*, 2006). A similar phenotype is observed when *Notch1* and/or *Notch2* are ablated in the melanocyte lineage; the severity of the hair-graying phenotype depends on the number of inactivated *Notch* alleles (Schouwey *et al.*, 2007).

This study was designed to determine whether Notch signaling is required for other steps of melanocyte lineage postnatal development and biology than MSCs maintenance. For this purpose, we re-investigated the phenotype of conditional *Rbp-J* knockout (KO) mice using the *Tg(Dct-lacZ)* reporter transgene (MacKenzie *et al.*, 1997). We observed that the number and distribution of cells of the melanocyte lineage are impaired in the HFs of conditional *Rbp-J* KO mice. Moreover, Notch/RBP-J-deficient MBs and melanocytes are found in ectopic locations relative to the outer root sheath and hair matrix, respectively. Finally, Notch/RBP-J-deficient MSCs and MBs undergo precocious differentiation into fully mature, pigmented melanocytes in the LPP, whereas MBs are in reduced number and remain undifferentiated in the hair matrix. Thus, Notch/RBP-J signaling plays a role in maintaining MSCs and their MB progeny in an undifferentiated state.

RESULTS

Coat color dilution in Notch/RBP-J-deficient mice

To investigate the roles of the Notch pathway in melanocyte lineage postnatal development, we conditionally ablated Notch signaling in the melanocyte lineage of mice. For this purpose, we used the same conditional mutant as used by Moriyama *et al.* (2006). This mutant carries two floxed *Rbp-J*^{f} alleles (Han *et al.*, 2002) and the *Tg(Tyr-Cre)1Lru* transgene (Delmas *et al.*, 2003), and is referred to as *cRBP-J* KO for conditional *RBP-J* KO in the rest of this paper. In *cRBP-J* KO mice, Cre recombinase is active from embryonic day 11.5 (E11.5) onwards (Delmas *et al.*, 2003). To follow the melanocyte lineage in c*RBP-J* KO mice, we took advantage of the *Tg(Dct-lacZ)* reporter transgene that allows identification of MBs and melanocytes by X-Gal staining (MacKenzie *et al.*, 1997). This reporter can be used to monitor cells of the melanocyte lineage in c*RBP-J* KO mice, since *Dct*-promoter activity is not decreased when Notch signaling is blocked (Kumano *et al.*, 2008). We studied the coat-color phenotype of *cRBP-J* KO; *Tg(Dct-lacZ)* and control mice. At postnatal day 8 (P8), *cRBP-J* KO*; Tg(Dct-lacZ)* mice had a diluted coat color (Figure 1a). At P30, coat color was further diluted (Figure 1b) and turned white within a few months (data not shown). The penetrance of the conditional RBP-J mutation was complete, independent of genetic background. This age-dependent coat-color whitening was identical to that of c*RBP-J* KO mice that do not carry the *Dct-lacZ* transgene (Moriyama *et al.*, 2006, and our own observations).

The number of melanoblasts is reduced in *cRBP-J* KO; *Tg(Dct-lacZ)* postnatal HFs

We isolated HFs from the skin of *cRBP-J* KO*; Tg(Dct-lacZ)* and *Tg(Dct-lacZ)* control mice and counted β-galactosidase (β-gal)-positive cells within the HFs, excluding the hair matrix where they were not countable. Indeed, in the hair matrix, the density of β-gal-positive cells was very high and the X-Gal precipitate leaked so that the boundaries of individual β-gal-positive cells were not visible. No X-Gal staining could be detected in HFs from the skin of *cRBP-J* KO and *Rbp-J*$^{f/f}$ mice lacking the *Dct-lacZ* transgene, indicating that the *lacZ* reporter under the control of the *Dct* promoter is a robust and reliable marker of melanoblasts within the HF (Figure S1). We analyzed HFs at both P8 and P30 that corresponded to the anagen of the first and second hair cycles, respectively. In P8 control HFs (Figure 1c), the average number of β-gal-positive cells per HF was 5.6 ± 2.5 ($n = 47$ HFs). In P8 *cRBP-J* KO*; Tg(Dct-lacZ)* HFs (Figure 1d), the count was 1.8 ± 1.6 ($n = 124$ HFs). The number of β-gal-positive cells was significantly reduced in *cRBP-J* KO*; Tg(Dct-lacZ)* HFs as compared with that in *Tg(Dct-lacZ)* controls (Mann–Whitney *U*-test, $P < 10^{-4}$). In P30 control HFs (Figure 1e), the average number of β-gal-positive cells per HF was 6.2 ± 2.5 ($n = 84$ HFs). In P30 *cRBP-J* KO*; Tg(Dct-lacZ)* HFs (Figure 1f), the count was 1.2 ± 1.3 ($n = 162$). The number of β-gal-positive cells was significantly reduced in *cRBP-J* KO; *Tg(Dct-lacZ)* HFs as compared with that in *Tg(Dct-lacZ)* controls (Mann–Whitney *U*-test, $P < 10^{-4}$). At P8 and P30, in both controls and mutants the number of β-gal-positive cells was not noticeably different between HFs producing guard, auchene, awl, or zigzag hair shafts.

We compared the mean number of β-gal-positive cells per HF at P8 and P30. In *Tg(Dct-lacZ)* control HFs, there was no difference in the mean number of β-gal-positive between P8 and P30 (Mann–Whitney *U*-test). By contrast, in *cRBP-J* KO*; Tg(Dct-lacZ)* HFs the mean number of β-gal-positive cells was lower at P30 than at P8 (Mann–Whitney *U*-test, $P < 10^{-3}$).

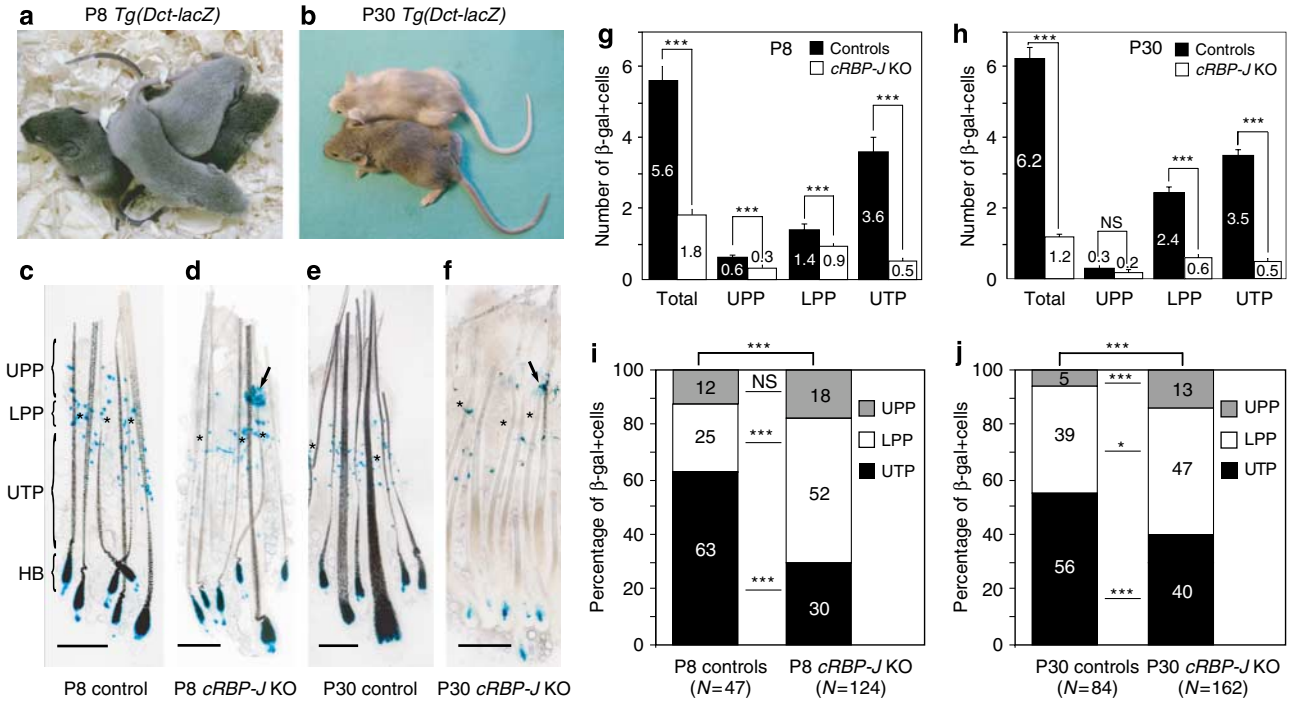

Figure 1. Coat-color phenotype and distribution of β-gal-positive cells in *cRBP-J* KO; *Tg(Dct-lacZ)* and control HFs at P8 and P30. (**a**) Coat-color phenotype of two 8-day-old (P8) *cRBP-J* KO; *Tg(Dct-lacZ)* pups (middle) and two *Tg(Dct-lacZ)* control littermates (sides). (**b**) Thirty-day-old (P30) *cRBP-J* KO; *Tg(Dct-lacZ)* mouse (top) and *Tg(Dct-lacZ)* control littermate (bottom). (**c**–**f**) HFs were dissected after X-Gal staining of the skin; asterisks indicate the position of the LPP. Bars = 200 μm. (**c**) HFs from a P8 *Tg(Dct-lacZ)* control mouse; parentheses show the location for the UPP, LPP, UTP, and HB on the HF situated on the left. (**d**) HFs from a P8 *cRBP-J* KO; *Tg(Dct-lacZ)* mouse; the arrow points at a dendritic β-gal-positive cell. (**e**) HFs from a P30 *Tg(Dct-lacZ)* control mouse; the hair clubs from the first hair cycle are still present, allowing location of LPP (asterisks). (**f**) HFs from a P30 *cRBP-J* KO; *Tg(Dct-lacZ)* mouse; the arrow points at a dendritic and pigmented β-gal-positive cell. (**g**–**h**) Means of the number of β-gal-positive cells in the *Tg(Dct-lacZ)* control (black histograms) and *cRBP-J* KO; *Tg(Dct-lacZ)* (white histograms) HFs, UPP, LPP, and UTP at P8 (**g**) and P30 (**h**). The total corresponds to the sum of β-gal-positive cells mean numbers in the UPP, LPP, and UTP. Means for the considered region are given rounded to the nearest tenth either on or above each histogram. Bars represent SEM. Data were analyzed using Mann–Whitney tests: $***P<10^{-3}$; NS, non-significant. (**i**, **j**) Distribution patterns of β-gal-positive cells in HFs according to their location (black, UTP; white, LPP; gray, UPP) at P8 (**i**) and P30 (**j**); to the left: distributions in *Tg(Dct-lacZ)* control HFs; to the right: distributions in *cRBP-J* KO; *Tg(Dct-lacZ)* HFs. Distributions are given as percentages of total cell counts. Numbers of HFs analyzed are given as *N* under each histogram. Numbers drawn on histograms are the percentages for the considered parts. Data were analyzed using χ^2-tests for overall distributions (asterisks above the histograms) or Fisher's exact tests for percentages in a given part (asterisks between the histograms); $***P\leqslant10^{-3}$; $*P\leqslant0.05$; NS, non-significant.

Altogether, these results show that the number of MBs is reduced in the HFs of c*RBP-J* KO mice at both P8 and P30 as compared with that in control mice. Moreover, whereas the number of MBs remains constant between the first and second hair cycles in the HFs of control mice, it dwindles significantly in the HFs of c*RBP-J* KO mice.

Absence of Notch signaling alters distribution of melanoblasts in postnatal HFs

We examined whether the reduced number of β-gal-positive cells in *cRBP-J* KO; *Tg(Dct-lacZ)* HFs was homogenous or could be attributed to a specific region of the HF. To this end, we split each HF in four parts corresponding to anatomically distinct regions of the follicle: (i) the upper permanent part (UPP), from the epidermis to the bulge; (ii) the LPP, the bulge where the MSCs reside; (iii) the upper transitory part (UTP), from the LPP to the bulb; and (iv) the hair bulb (HB) (Figure 1c). The LPP or bulge is located at the insertion of the arrector pili muscle (Muller-Rover *et al.*, 2001). It extends from the lower part of the insertion site of the arrector pili muscle to the opening of the sebaceous gland duct (Paus *et al.*, 1999; Tiede *et al.*, 2007). In HFs where these marks were visible, the lower part of the insertion of the arrector pili muscle was situated at the junction of the dermis and the subcutis, and the LPP covered 120 μm on average. Therefore, in HFs where the arrector pili and/or the opening of the sebaceous gland were not visible, the lower boundary for the LPP was chosen at the junction of the dermis and the subcutis, and its upper boundary 120 μm above. We counted the numbers of β-gal-positive cells in the three upper parts for each HF; β-gal-positive cells within the HB were not countable. We compared the mean numbers of β-gal-positive cells in each part between *Tg(Dct-lacZ)* control and *cRBP-J* KO; *Tg(Dct-lacZ)* HFs (Figure 1g and h). At P8, the means of β-gal-positive cells were significantly lower in *cRBP-J* KO; *Tg(Dct-lacZ)* UPP, LPP, and UTP than in controls (Mann–Whitney tests, all $P<10^{-3}$) (Figure 1g). At P30, the mean numbers of β-gal-positive cells in all parts, except UPP, were significantly lower in *cRBP-J* KO; *Tg(Dct-lacZ)* than in controls (Mann–Whitney tests, $P<10^{-3}$, except for the UPP where *P*-value was not significant) (Figure 1h).

We then tested whether distribution of β-gal-positive cells was the same in *Tg(Dct-lacZ)* control and *cRBP-J* KO*; Tg(Dct-lacZ)* HFs. To this end, we summed up the cell counts of each part and compared the overall distribution and percentages of β-gal-positive cells in each part between *Tg(Dct-lacZ)* controls and *cRBP-J* KO*; Tg(Dct-lacZ)* HFs (Figure 1i and j). At both P8 and P30, we found that the distributions of β-gal-positive cells in whole HFs were differing between mutants and controls (χ^2-test, $P<10^{-4}$ for both tests) (Figure 1i and j). At P8, we found a significantly higher percentage of β-gal-positive cells in the LPP and a lower percentage in the UTP in *cRBP-J* KO*; Tg(Dct-lacZ)* HFs as compared with that in *Tg(Dct-lacZ)* control HFs (Fisher's exact tests, $P=10^{-3}$ and $P<10^{-4}$, respectively) (Figure 1i). In other words, in *Tg(Dct-lacZ)* control HFs, most of the β-gal-positive cells were found in the UTP, whereas in *cRBP-J* KO*; Tg(Dct-lacZ)* HFs, most of them were found in the LPP (Figure 1i). At P30, the percentages of β-gal-positive cells were higher in the LPP and UPP, but lower in the UTP of *cRBP-J* KO*; Tg(Dct-lacZ)* HFs when compared with that in *Tg(Dct-lacZ)* controls (Fisher's exact tests, $P=0.05$ in the LPP and $P<10^{-3}$ in the UPP and UTP) (Figure 1j).

In sum, at both P8 and P30, distribution of MBs is affected in the HFs of *cRBP-J*-KO mice. Notably, whereas there is a reduced number of MBs in the LPP of *cRBP-J* KO mice as compared with controls, the relative proportion of MBs is significantly increased in this specific region compared to controls at both time points.

Without Notch signaling, the LPP melanoblast pool is depleted between the first and the second hair cycle

The origin of HF melanocytes is different between the first and the second hair cycle. Indeed, during the first anagen, melanocytes differentiate directly from embryonic melanoblasts, whereas during the second anagen, they derive from the MSCs located in the LPP (Mak *et al.*, 2006). We tested whether this difference in melanocyte origin could result in changes in mean numbers and distributions of cells of the melanocyte lineage between the first and the second hair cycle. To this end, we compared the numbers of β-gal-positive cells and distributions at P8 and P30 in *Tg(Dct-lacZ)* control HFs. The average number of β-gal-positive cells was significantly increased in the LPP at P30 and significantly decreased in the UPP at P30 (Mann–Whitney tests, both $P<10^{-3}$) (Figure 1g and h, black histograms). Moreover, distribution in the entire HF was different between P8 and P30 mice (χ^2-test, $P<10^{-4}$) (Figure 1i and j, left panels). In *Tg(Dct-lacZ)* control HFs at P30, the percentage of β-gal-positive cells in the LPP was higher than at P8, at the expense of the UPP and UTP (Fisher's exact tests, $P<10^{-3}$ in the LPP and UPP, and $P=0.05$ in the UTP) (Figure 1i and j, left panels).

We then studied the evolution of numbers and distributions of β-gal-positive cells in *cRBP-J* KO*; Tg(Dct-lacZ)* HFs between the first and the second hair cycle. Mean numbers were significantly lower in whole HFs, UPP, and LPP at P30, but not different in the UTP (Mann–Whitney tests, all $P<10^{-3}$ except for the UTP where *P*-value was not significant) (Figure 1g and h, white histograms). The distribution in the entire HF was different between P8 and P30 (χ^2-test, $P<10^{-4}$) (Figure 1i and j). The difference was due to a significantly increased percentage of β-gal-positive cells in the UTP at P30 (Fisher's exact tests, $P=0.03$) (Figure 1i and j, right panels).

In conclusion, regarding the LPP, the mean number of β-gal-positive cells evolved differently in *Tg(Dct-lacZ)* control and *cRBP-J* KO; *Tg(Dct-lacZ)*: whereas it increased in controls, it diminished in mutants. These data suggest that the reduction in the number of MBs in *cRBP-J* KO*; Tg(Dct-lacZ)* HFs is mainly due to depletion of the LPP population.

Impaired terminal differentiation of Notch-deficient melanoblasts within the HB

In HBs, although β-gal-positive cells were not countable, we categorized the HB populations based on the presence or absence of X-Gal precipitate. We considered that an HB with some precipitate contained at least one β-gal-positive cell. We then asked whether there was a correlation between the presence of β-gal-positive cells in each HB and the corresponding hair shaft color. In *Tg(Dct-lacZ)* control HFs at P8, all HBs contained β-gal-positive cells (Figures 1c and 2a); the corresponding hair shafts were all fully pigmented (Figures 1c and 2b). In *cRBP-J* KO*; Tg(Dct-lacZ)* HFs at P8, whereas most HBs contained many β-gal-positive cells (Figures 1d and 2a), the corresponding hair shafts were fully pigmented (black), partially pigmented (gray), or even unpigmented (white) (Figures 1d and 2b). Surprisingly, in P8 *cRBP-J* KO*; Tg(Dct-lacZ)* HFs, white hairs were produced not only by HBs devoid of β-gal-positive cells, but also by HBs containing at least one β-gal-positive cell (Figure 2, compare panels a to b). It was even more striking at P30. Indeed, all control HBs at P30 contained β-gal-positive cells and produced fully pigmented hair shafts (Figures 1e and 2). By contrast, two-thirds of *cRBP-J* KO*; Tg(Dct-lacZ)* HBs still contained at least one β-gal-positive cell, whereas one-third was devoid of any β-gal-positive cell (Figure 2). In HBs containing β-gal-positive cells, there were fewer β-gal-positive cells than in controls, and almost all hair shafts were white (Figure 1f). However, despite presence of β-gal-positive cells in 67% of *cRBP-J* KO*; Tg(Dct-lacZ)* HBs, 98% of *cRBP-J* KO*; Tg(Dct-lacZ)* hairs were white, 2% gray, and none was black (Figure 2). In *cRBP-J* KO*; Tg(Dct-lacZ)* HBs containing β-gal-positive cells but producing white hair shafts, β-gal-positive cells were never pigmented, suggesting that they were MBs.

These observations suggest that without Notch signaling, at least some MBs can complete their migration from the LPP to the HB, but that terminal differentiation of MBs into functional, pigment producing melanocytes is impaired.

Anticipated differentiation of Notch/RBP-J-deficient melanoblasts within the HF

While investigating the effect of impaired Notch signaling on MBs number, we noticed an effect on the morphology of MB. In the control UPP, LPP, and UTP, at both P8 and P30 β-gal-positive cells were small, round, oval, or fusiform in shape,

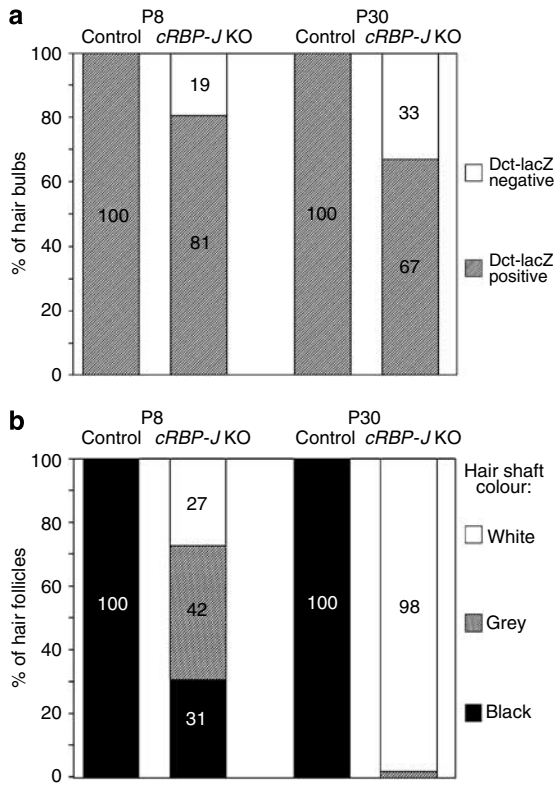

Figure 2. Impaired terminal differentiation of HB melanoblasts in *cRBP-J KO; Tg(Dct-lacZ)* HFs. (**a**) Proportion of HBs containing β-gal-positive cells (gray boxes) and devoid of β-gal-positive cells (white boxes) at P8 (left) and P30 (right). Dct-lacZ positive: HB with at least one β-gal-positive cell. Dct-lacZ negative: HB devoid of β-gal-positive cell. (**b**) Proportion of HFs producing black, gray, or white hair shafts. The HBs in panel (**a**) belong to the HFs in panel (**b**). Control: *Tg(Dct-lacZ)* control HFs ($n=47$ at P8; $n=84$ at P30); cRBP-J KO: *cRBP-J* KO*; Tg(Dct-lacZ)* HFs ($n=124$ at P8; $n=162$ at P30).

and were devoid of pigment (Figures 1c and e, and 3a, c, and e). By contrast, in P8 and P30 *cRBP-J* KO*; Tg(Dct-lacZ)* HFs, some β-gal-positive cells were big and dendritic, especially in the LPP and UPP; most of them were pigmented (Figures 1d and f, and 3b, d, and f). Such pigmented β-gal-positive cells were found in 20% of *cRBP-J* KO*; Tg(Dct-lacZ)* HFs (26/124 at P8 and 33/162 at P30). Most were found at the LPP level (16/26 at P8; 18/33 at P30). By contrast, no pigmented β-gal-positive cells were found in *Tg(Dct-lacZ)* control HFs at P8. Four only were found in the 84 *Tg(Dct-lacZ)* control HFs analyzed at P30, two in the LPP, and two in the UTP. The proportion of pigmented, β-gal-positive cells was significantly increased in *cRBP-J* KO*; Tg(Dct-lacZ)* HFs as compared with that in control HFs at both P8 and P30 (Fisher's exact test, $P=1.8\ 10^{-4}$ at P8 and $P=1.1\ 10^{-3}$ at P30). We examined whether pigmented cells occurred evenly in *cRBP-J* KO*; Tg(Dct-lacZ)* HFs or preferentially in a specific part. The proportion of pigmented, β-gal-positive cells was significantly higher in the *cRBP-J* KO*; Tg(Dct-lacZ)* LPP only (Fisher's exact test, $P=0.006$ at P8 and $P=0.024$ at P30; Figure 3g). To confirm that pigmented β-gal-positive cells were melanocytes, we used an antibody against Tyrosine-Related Protein 1 (TYRP1/TRP1). *Tyrp1* mRNA is expressed at low levels in MBs in the UTP and at higher levels in melanocytes in HB, but its expression is not detected in MSCs in the LPP (Osawa *et al.*, 2005). By immunofluorescence, we found cells strongly positive for TYRP1 in the UPP, LPP, and UTP of c*RBP-J* KO HFs; these TYRP1-positive cells were often pigmented (Figure 3h–k).

These experiments suggest that without Notch signaling, MBs undergo anticipated differentiation into melanocytes in the LPP.

Ectopic location of melanocytes in *cRBP-J*-KO HFs

While studying *cRBP-J* KO HFs, we noticed that some P8 and almost a fifth of P30 dermal papillae were pigmented (Figure 4a). No pigmentation was seen in such a location in control HFs. The pigment could have two origins, impaired secretory activity of melanosomes from the nearby hair matrix melanocytes or mislocation of melanocytes within the dermal papilla. To differentiate between these two possibilities, we looked for β-gal-positive cells in the dermal papillae of control and *cRBP-J* KO*; Tg(Dct-lacZ)* HFs at P30. As expected, no β-gal-positive cells were seen in control dermal papillae (84 dermal papillae analyzed) (Figure 4b). By contrast, 26/162 (16%) dermal papillae from *cRBP-J* KO*; Tg(Dct-lacZ)* HFs contained β-gal-positive cells (Figure 4c–e). Such β-gal-positive cells were observed in dermal papillae from both pigmented and unpigmented *cRBP-J* KO*; Tg(Dct-lacZ)* HFs (Figure 4d and e, respectively). We then investigated whether such misplaced β-gal-positive cells could be seen in other locations. Indeed, we observed β-gal-positive cells at various areas of *cRBP-J* KO*; Tg(Dct-lacZ)* skin at P30: in the dermis, often close to the LPP (5/162 HFs) (Figure 4f), within the club hair from the first hair cycle (16/162 HFs) (Figure 4g), surrounding the hair shaft (20/162 HFs) (Figure 4f and h), or outside the ORS (6/162) (Figure 4i). β-gal-positive cells were never found in such areas in controls. To assess the location of the β-gal-positive cells found in the dermis in the vicinity of the ORS, we performed immunofluorescence staining with an antibody against keratin-5, which is expressed in ORS keratinocytes (Kaufman *et al.*, 2003). Pigmented cells were found outside of the keratin-5-expressing layer (Figure 4j and k).

These observations indicate that Notch signaling is involved in retaining undifferentiated MBs within the ORS of HFs, and differentiated melanocytes within the hair matrix, and in preventing migration of both MBs and melanocytes to ectopic locations.

DISCUSSION

Lack of Notch signaling affects the number and distribution of melanoblasts within the HFs

Dissection of X-Gal-stained *Tg(Dct-lacZ)* HFs allowed us to study the distribution pattern of MBs in HFs. Indeed, this technique makes it possible to visualize the entire set of melanocyte lineage cells in a given HF, which would be very difficult to accomplish with histological sections.

Both mean numbers and distribution patterns of MBs are different in c*RBP-J* KO HFs as compared with control HFs. Our data confirm those of Moriyama *et al.* (2006): the

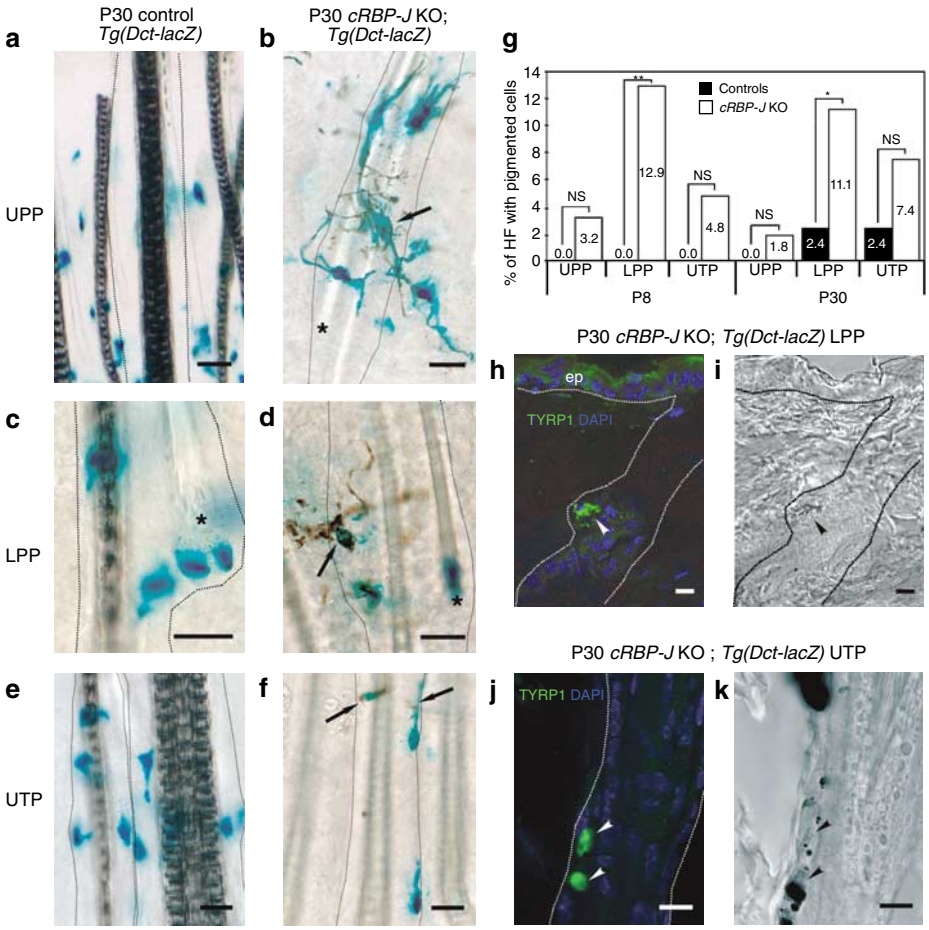

Figure 3. Anticipated differentiation of melanoblasts in cRBP-J KO; Tg(Dct-lacZ) HFs. (**a**–**f**) Parts of *Tg(Dct-lacZ)* control (**a**, **c**, **e**) and *cRBP-J* KO*; Tg(Dct-lacZ)* (**b**, **d**, **f**) HFs; control and mutant UPP (**a**, **b**), LPP (**c**, **d**) and UTP (**e**, **f**). HFs were dissected after X-Gal staining of the skin. Stars indicate the base of hair clubs from the first hair cycle. Arrows point at pigment within β-gal-positive cells. Dotted lines delimit the HF. (**g**) Percentages of HFs with β-gal-positive, dendritic, and/or pigmented cells in the UPP, LPP, or UTP at P8 (left panel) and P30 (right panel). Number of HFs analyzed are 47 and 124 at P8 and 84 and 162 at P30 for *cRBP-J* KO*; Tg(Dct-lacZ)* and *Tg(Dct-lacZ)* controls, respectively. Asterisks correspond to the *P*-value for Fisher's exact test; **P*<0.05; ***P*<0.01; NS, non-significant. (**h**–**k**) Immunofluorescence staining of P30 *cRBP-J* KO*; Tg(Dct-lacZ)* skin sections using anti-TYRP1 antibody (green) and 4,6-diamidino-2-phenylindole (blue); (**h**) optic section in LPP; ep, epidermis, with nonspecific TYRP1 labeling in keratinocytes; (**j**) optic section in UTP; panels (**i**) and (**k**) are the Nomarski pictures of images in panels (**h**) and (**j**), respectively; arrowheads point at the same cells in fluorescent and Nomarski pictures. Sections thickness, 0.5 μm. Bars = 20 μm in panels (**a**)–(**f**) and 10 μm in panels (**h**)–(**k**).

number of c*RBP-J* KO MBs is reduced in the whole HF, and MBs are especially depleted in the LPP. Moreover, they show that the percentage of MBs in the LPP is increased in c*RBP-J*-KO HFs at both P8 and P30. This overrepresentation of MBs within the LPP may reflect one or several of the following defects: (1) a reduced ability of MSCs to generate MBs, (2) an impaired ability of MBs to emigrate from the LPP, and (3) an impaired proliferation and/or survival of MBs within the UTP. Although these possibilities should be addressed in future studies, our observations show that the role of Notch signaling on HF MBs is not limited to maintenance of the MSC pool.

Absence of Notch signaling impairs the timing of melanoblast differentiation within the HFs

Our data further indicate that inactivation of Notch signaling is associated with precocious expression of the melanogenic enzyme TRP1 and with the anticipated synthesis of melanin in MBs located in the three upper regions of the HF, the LPP, UTP, and UPP. These observations indicate that Notch signaling prevents differentiation of MBs into melanocytes in these regions. Such a function for Notch has recently been reported in the embryonic development of limb muscles. Indeed, in the absence of *RBP-J*, myogenic progenitor cells differentiate in an uncontrolled and premature manner at E11.5. Consequently, the progenitor pool is depleted and the satellite cell population is missing at E18.5 (Vasyutina *et al.*, 2007). Strikingly, during postnatal myogenesis, Notch signaling maintains PAX3-positive myogenic precursors in an undifferentiated state through upregulation of *Pax3* and downregulation of muscular differentiation genes (Conboy and Rando, 2002). A similar mechanism may well operate in MSCs that have been shown to express PAX3 as myogenic precursors do (Osawa *et al.*, 2005).

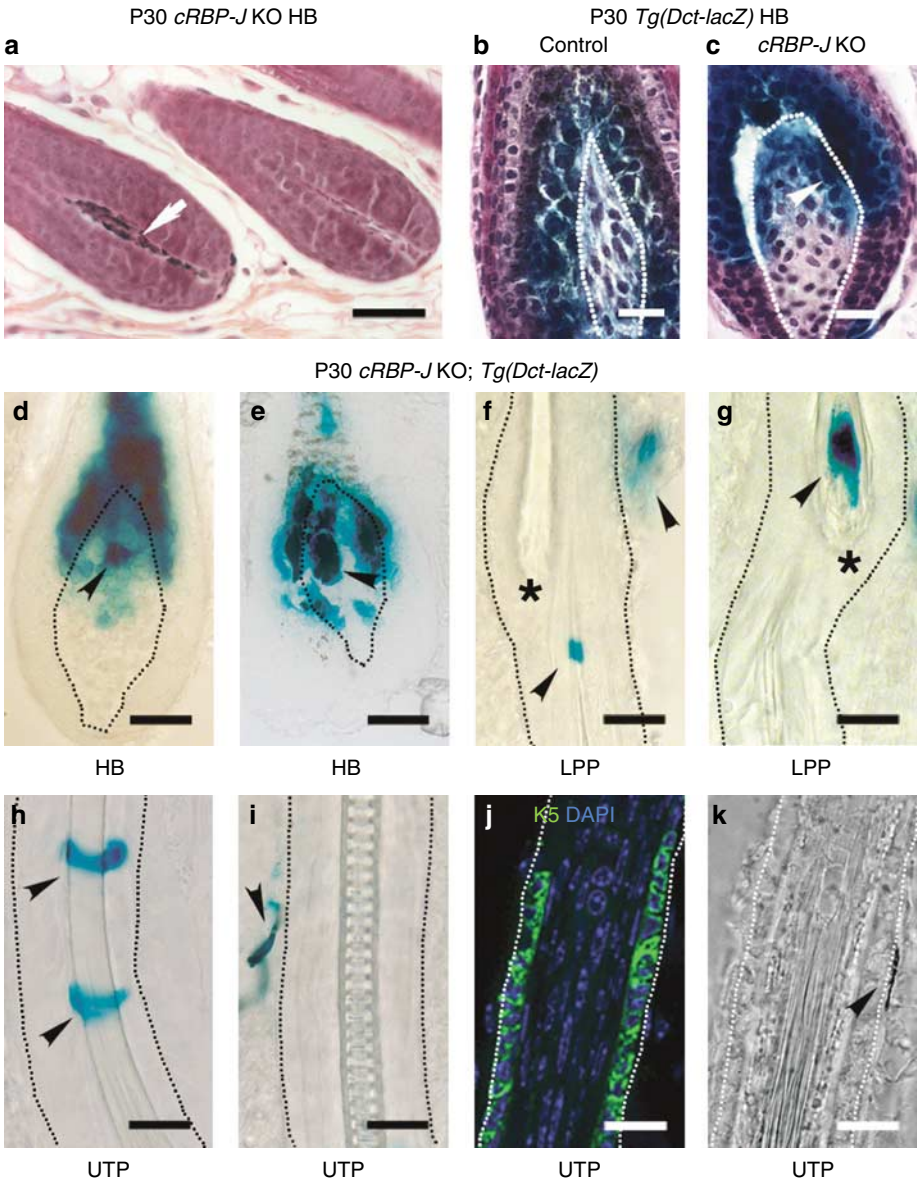

Figure 4. Ectopic location of melanoblasts in cRBP-J KO; Tg(Dct-lacZ) HFs. (**a**) Histological section of P8 *cRBP-J* KO skin. The arrow points at pigment within the dermal papilla. (**b**, **c**) Histological sections of P30 *Tg(Dct-lacZ)* control (**b**) and *cRBP-J* KO; *Tg(Dct-lacZ)* (**c**) HB; skins were stained with X-Gal before sectioning. Dotted lines delimit the dermal papilla; white arrowhead points at a β-gal-positive cell within the dermal papilla. (**d**–**i**) Parts of P30 *cRBP-J* KO*; Tg(Dct-lacZ)* HFs: HB (**d**, **e**), LPP (**f**, **g**), UTP (**h**, **i**); the corresponding skins were stained with X-Gal and HFs were dissected. Dotted lines delimit the dermal papilla in panels (**d**) and (**e**) and the ORS in panels (**f**)–(**i**). Asterisks indicate the base of hair clubs from the first hair cycle. Arrowheads point at ectopic β-gal-positive cells. (**j**) Immunofluorescence staining of a P30 *cRBP-J* KO*; Tg(Dct-lacZ)* UTP using anti-K5 antibody (green) and 4,6-diamidino-2-phenylindole (blue). (**k**) Nomarski picture of the same section as in panel (**j**). Dotted lines delimit the ORS, arrowhead points at a pigmented cell outside the ORS. Sections thickness: 10 μm in panels (**a**)–(**c**); 0.5 μm in panels (**j**) and (**k**). Bars = 50 μm in panel (**a**); 20 μm in panels (**b**), (**c**), and (**f**)–(**k**); 40 μm in panels (**d**) and (**e**).

Our results indicate that the proportion of pigmented melanocytes is significantly higher in the LPP but not in the UPP and UTP of *cRBP-J* KO HFs as compared with controls. As the LPP contains the MSCs as well as early MBs, one explanation for this observation could be that Notch activation acts specifically on MSCs and early MBs to maintain them in an undifferentiated state. Consequently, Notch-deficient melanocytes within the LPP would be insensitive to the migrating cues that attract MBs out of the LPP toward the HB. The depletion of the MSC pool could be a consequence of the anticipitated differentiation of MSCs into melanocytes. However, the anticipated differentiation into melanocytes occurs in a small percentage of the *cRBP-J* KO LPP (12.9 and 11.1% at P8 and P30, respectively), whereas depletion of the MSC population within the *cRBP-J* KO LPP is a general event. Thus, if the anticipated differentiation contributes to depletion of the MSC pool in the *cRBP-J* KO LPP, it cannot account for all of it. We conclude that depletion of the MSC pool in the *cRBP-J* KO LPP is a consequence of at least two events that are not necessarily

interrelated, MSC apoptosis as shown by Moriyama *et al.* (2006) and anticipated differentiation. Strikingly, in control HFs, whereas no differentiated melanocytes are detected in the UPP, LPP, and UTP at P8, some are found in the LPP and UTP at P30, although very rarely.

Notch/RBP-J-deficient melanoblasts are in reduced number and lack terminal differentiation within the HBs

Many c*RBP-J* KO HFs cannot produce pigmented hair shafts despite presence of MBs within the hair matrix. These MBs, that are neither dendritic nor pigmented, stay undifferentiated in a region where terminal differentiation occurs in wild-type HFs. This is particularly true at P30 during the second hair cycle when Notch/RBP-J-deficient MBs are in reduced number in the HB. The absence of differentiation may be directly linked to the lack of Notch signaling in MBs within the HBs. Alternatively, absence of differentiation may be an indirect consequence of the lack of Notch signaling in MBs in the LPP and UTP, leading to the reduced number of HB MBs. Indeed, in wild-type conditions, differentiation of MBs into pigment-producing melanocytes in the HB may require a critical number of MBs. Thus, presence of DCT-positive, unpigmented cells in c*RBP-J* KO HBs producing white hair shafts could be a consequence of the reduction in the number of MBs reaching the HB, and not of the absence of Notch signaling in HB MBs *per se*. Whatever the reason, Notch signaling acts either directly or indirectly on terminal differentiation of MBs within the HB.

Notch/RBP-J-deficient melanoblasts and melanocytes are found in ectopic locations in the skin

MBs and melanocytes are observed in various ectopic locations in the skin of *cRBP-J* KO mice. We assume that MBs and melanocytes migrated to inappropriate locations due to lack of Notch signaling. Indeed, Notch signaling could participate in the communication between MBs and keratinocytes. In c*RBP-J* KO mice, such communication would be disrupted eventually leading to altered MB migration. However, many HBs of c*RBP-J* KO mice contain MBs, indicating that most RBP-J-deficient MBs are still able to reach the hair matrix. Thus, altered migration is only a minor phenotype in Notch/RBP-J-deficient MBs.

Most of the DCT-positive cells seen in ectopic position were pigmented. It raises the possibility that improper migration occurs whenever an RBP-J-deficient MB undergoes precocious differentiation in the LPP, UPP, and UTP. Alternatively, within wild-type HFs, the environment may inhibit differentiation of MBs into pigment-producing melanocytes; when they are out of their normal environment, RBP-J-deficient MBs would escape the inhibiting signals and differentiate into mature melanocytes.

We conclude that Notch signaling fulfills multiple roles in the melanocyte lineage of postnatal HFs (Figure 5). Notch activity is required not only to maintain MSCs in the LPP, but also to prevent MBs differentiation in the UPP, LPP, and UTP, and to control proper migration of MBs from the LPP to their final location within the HB. Finally, Notch signaling is required, either directly or indirectly, for terminal differentiation of MBs into melanin-producing melanocytes (Figure 5). Determining the target genes for Notch pathway in the melanocyte lineage will be the objective of further studies.

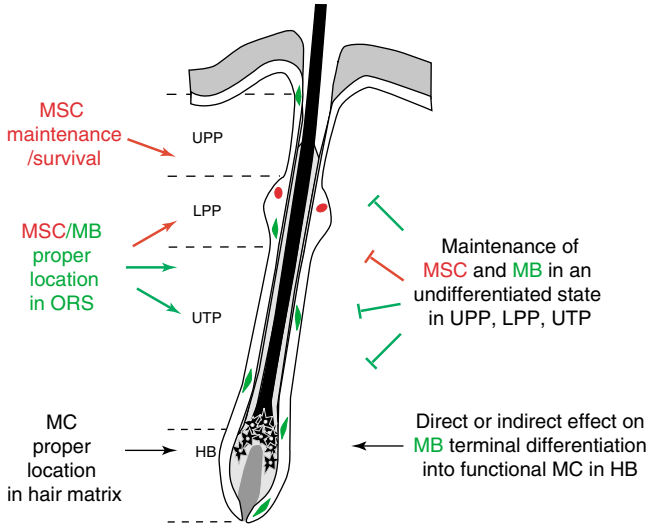

Figure 5. Roles of Notch signaling in postnatal development of the melanocyte lineage. Schematic representation of an anagen HF. Red, green, and black lines denote roles on MSCs, MBs, and melanocytes (MC), respectively. Ends of lines are either arrowheads indicating a positive action or perpendicular lines indicating an inhibitory action for Notch signaling.

MATERIALS AND METHODS

Animals

Rbp-J^{f} mice were obtained from the facility of Kyoto University. *Tg(Tyr-Cre)1Lru* mice were obtained from the facility of Institut Curie. *Tg(Dct-lacZ)* mice were obtained from Western General Hospital, Edinburgh. Mice were bred and crossed in our facility. Animal care and use were approved by the ethical committee of Alfort Veterinary in compliance with the European Union Standards. Mutant mice used were *Tg(Tyr-Cre)1Lru/°*; *Rbp-J*$^{f/f}$ males or *Tg(Tyr-Cre)1Lru/Tg(Tyr-Cre)1Lru*; *Rbp-J*$^{f/f}$ females. Control mice were littermates either transgenic for *Tg(Tyr-Cre)1Lru* and carrying no or only one *Rbp*^{f} allele, or mice non-transgenic for *Tg(Tyr-Cre)1Lru*.

Genotyping

To identify *Rbp-J* wild-type allele, *Tg(Tyr-Cre)1Lru*, and *Tg(Dct-lacZ)* transgenes, PCRs were performed as previously described (Han *et al.*, 2002; Delmas *et al.*, 2003; Takemoto *et al.*, 2006). *Rbp-J*^{f} allele was amplified using the following primers: *Rbp-J*^{f} forward: 5′-gttc ttaacctgttggtcggaacc-3′; *Rbp-J*^{f} reverse: 5′-gggctgctaaagcgcatgct-3′. PCR conditions were 30 seconds at 94 °C, 30 seconds at 52 °C, 40 seconds at 72 °C for 35 cycles, and a final extension at 72 °C for 10 minutes. The *Rbp-J*^{f} PCR fragment was 150 bp long.

Histology and X-Gal staining

Dorsal skin was fixed in 4% paraformaldehyde at 4 °C for 45 minutes. X-Gal staining was performed as previously described (Aubin-Houzelstein *et al.*, 1998). For cryostat sectioning, samples were embedded in Tissue-Tek OCT Compound (Electron Microscopy Sciences, Hatfield, PA), frozen, sectioned with a cryostat (10-μm), and counterstained with nuclear red. For standard

histology, skin samples were fixed overnight in 4% formaldehyde/phosphate-buffered saline (PBS) at 4 °C, embedded in paraffin, sectioned (4-μm) following standard procedures, and counterstained with hemalun–eosin.

Hair follicles dissection

Dorsal skin was dissected from two P8 and three P30 *Tg(Dct-lacZ)* controls, and three P8 and three P30 *cRBP-J KO; Tg(Dct-lacZ)* mice. The skin was fixed in 4% paraformaldehyde at 4 °C for 45 minutes, rinsed in PBS, then cut in smaller pieces. For each mouse, three groups of small skin pieces were kept: the first was obtained from the anterior part of the dorsal skin sample, in the forelimb region; the second from the middle part of the sample; and the third came from the posterior part of the sample, from the hind-limb region. The small pieces were stained with X-Gal for 48 hours at 32 °C. Individual HFs were isolated from the X-Gal-stained small pieces under a binocular microscope. The isolated HFs were mounted in Mowiol (Polysciences Europe, Eppelheim, Germany).

β-Gal-positive-cell counting and statistical analyses

β-Gal-positive cells from individual HFs were counted under microscope. The HFs were obtained from two *cRBP-J* KO*; Tg(Dct-lacZ)* and three *Tg(Dct-lacZ)* control littermates at P8, and three *cRBP-J* KO*; Tg(Dct-lacZ)* and three *Tg(Dct-lacZ)* control littermates at P30. A comparable number of HFs was analyzed from each mouse. The lower boundary for the LPP was anatomically located at the junction of the dermis and the subcutis. In P30 HFs, it corresponded to the base of the hair club from the first hair cycle. The upper boundary for LPP was defined as the opening of the sebaceous gland when visible, or placed 120 μm above the lower boundary otherwise. Statistical analyses were performed with StatViewF-4.51.3.PPC software from Abacus Concepts (Berkeley, CA). Data are expressed as means ± SD. Distribution normality was tested by comparing the observed distribution with a normal distribution with the same mean and SD, and using a Kolmogorov–Smirnov test. Variances were compared with an *F*-test. Means were compared with Student's *t*-test for normally distributed values with equal variances, and with a Mann–Whitney *U*-test otherwise. Distributions were compared with a χ^2-test. Percentages were compared with an Fisher's exact test.

Immunofluorescence

Cryostat sections were rinsed in PBS. Blocking was performed in 10% normal goat serum in PBS for 1 hour at room temperature. Sections were incubated overnight at 4 °C in primary antibody solution (1:500 rabbit anti-mouse TYRP1/TRP1 antiserum; a kind gift from Vincent Hearing) or 1:1,000 rabbit anti-mouse K5 (Covance, Princeton, NJ) in 0.1% Tween-20 in PBS, and then for 1 hour at room temperature in goat anti-rabbit IgG Alexa Fluor 488 (Invitrogen, Cergy-pontoise, France) diluted 1:500 in 0.1% Tween-20 in PBS. 4,6-Diamidino-2-phenylindole was used for visualizing cell nuclei. Between two incubation steps, the sections were washed in 0.1% Tween-20 in PBS for 10 minutes. The sections were mounted in Vectashield (Vector Laboratories, Peterborough, UK).

Image acquisition

Bright-field and fluorescence microscopy were performed with a Zeiss Axioplan 2 Imaging microscope with ApoTome (upright stand), using Plan-NEOFLUAR (×10, ×25, and ×40 magnification) or Plan-APOCHROMAT (×63 and ×100 magnification) objective lenses with 0.3, 0.8, 1.3, 1.4, and 1.4 numerical apertures, respectively. Images were acquired with either an Axiocam HRc (color imaging) or an Axiocam MRm (fluorescence imaging) camera (Zeiss, Göttingen, Germany) coupled to Zeiss Axiovision 4.4 software. Minimal image processing was performed with Adobe Photoshop.

CONFLICT OF INTEREST

The authors state no conflict of interest.

ACKNOWLEDGMENTS

We are grateful to T Honjo, I Jackson, and V Hearing for the kind gift of the *RBPJ*^{f} mouse, the *Tg(Dct-lacZ)* mouse, and the TRP1 antiserum, respectively; and Y Barrandon for his protocol for HF dissection. We thank A Casanova, ML Daupin, and C Koenen for dedicated animal husbandry; A Champeix and P Wattier for histological work; L Guillaud and P Salaün for technical help; Marie-Anne Nicola and Emmanuelle Perret from the Plateforme d'Imagerie Dynamique at the Institut Pasteur for help with imaging; D Houzelstein for help with artwork; and M Chodkiewicz, M Cohen-Tannoudji, G Egidy-Maskos, X Montagutelli, and L Tiret for critical comments on the paper. GAH, FB, JDZ, and JJP were supported by the Association pour la Recherche contre le Cancer (ARC) (Grants 4332 and 99/7468) and by an agreement between the INRA and the Institut Pasteur; GAH and JJP were supported by the Grand Programme Horizontal ''Cellules Souches'' of the Institut Pasteur; VD and LL were supported by the Ligue Nationale contre le Cancer (Equipe Labellisée). JDZ was funded by the French Ministère de la Recherche et Nouvelles Technologies. This paper is dedicated to Charles Babinet.

SUPPLEMENTARY MATERIAL

Figure S1. X-Gal staining on isolated HFs from *Tg(Dct-lacZ)* and control mice.

REFERENCES

Artavanis-Tsakonas S, Matsuno K, Fortini ME (1995) Notch signaling. *Science* 268:225–32

Artavanis-Tsakonas S, Rand MD, Lake RJ (1999) Notch signaling: cell fate control and signal integration in development. *Science* 284:770–6

Aubin-Houzelstein G, Bernex F, Elbaz C, Panthier JJ (1998) Survival of patchwork melanoblasts is dependent upon their number in the hair follicle at the end of embryogenesis. *Dev Biol* 198:266–76

Bolos V, Grego-Bessa J, de la Pompa JL (2007) Notch signaling in development and cancer. *Endocr Rev* 28:339–63

Botchkareva NV, Khlgatian M, Longley BJ, Botchkarev VA, Gilchrest BA (2001) SCF/c-kit signaling is required for cyclic regeneration of the hair pigmentation unit. *FASEB J* 15:645–58

Chiba S (2006) Notch signaling in stem cell systems. *Stem Cells* 24:2437–47

Conboy IM, Rando TA (2002) The regulation of Notch signaling controls satellite cell activation and cell fate determination in postnatal myogenesis. *Dev Cell* 3:397–409

Delmas V, Martinozzi S, Bourgeois Y, Holzenberger M, Larue L (2003) Cre-mediated recombination in the skin melanocyte lineage. *Genesis* 36:73–80

Han H, Tanigaki K, Yamamoto N, Kuroda K, Yoshimoto M, Nakahata T *et al.* (2002) Inducible gene knockout of transcription factor recombination signal binding protein-J reveals its essential role in T *versus* B lineage decision. *Int Immunol* 14:637–45

Hurlbut GD, Kankel MW, Lake RJ, Artavanis-Tsakonas S (2007) Crossing paths with Notch in the hyper-network. *Curr Opin Cell Biol* 19: 166–75

Kato H, Sakai T, Tamura K, Minoguchi S, Shirayoshi Y, Hamada Y *et al.* (1996) Functional conservation of mouse Notch receptor family members. *FEBS Lett* 395:221–4

Kaufman CK, Zhou P, Pasolli HA, Rendl M, Bolotin D, Lim KC *et al.* (2003) GATA-3: an unexpected regulator of cell lineage determination in skin. *Genes Dev* 17:2108–22

Kumano K, Masuda S, Sata M, Saito T, Lee SY, Sakata-Yanagimoto S *et al.* (2008) Both Notch1 and Notch2 contribute to the regulation of melanocyte homeostasis. *Pigment Cell Melanoma Res* 21:70–8

Lang D, Lu MM, Huang L, Engleka KA, Zhang M, Chu EY *et al.* (2005) Pax3 functions at a nodal point in melanocyte stem cell differentiation. *Nature* 433:884–7

MacKenzie MA, Jordan SA, Budd PS, Jackson IJ (1997) Activation of the receptor tyrosine kinase Kit is required for the proliferation of melanoblasts in the mouse embryo. *Dev Biol* 192:99–107

Mak SS, Moriyama M, Nishioka E, Osawa M, Nishikawa S (2006) Indispensable role of Bcl2 in the development of the melanocyte stem cell. *Dev Biol* 291:144–53

Moriyama M, Osawa M, Mak SS, Ohtsuka T, Yamamoto N, Han H *et al.* (2006) Notch signaling via Hes1 transcription factor maintains survival of melanoblasts and melanocyte stem cells. *J Cell Biol* 173:333–9

Muller-Rover S, Handjiski B, van der Veen C, Eichmuller S, Foitzik K, McKay IA *et al.* (2001) A comprehensive guide for the accurate classification of murine hair follicles in distinct hair cycle stages. *J Invest Dermatol* 117:3–15

Nishimura EK, Jordan SA, Oshima H, Yoshida H, Osawa M, Moriyama M *et al.* (2002) Dominant role of the niche in melanocyte stem-cell fate determination. *Nature* 416:854–60

Osawa M, Egawa G, Mak SS, Moriyama M, Freter R, Yonetani S *et al.* (2005) Molecular characterization of melanocyte stem cells in their niche. *Development* 132:5589–99

Paus R, Muller-Rover S, Van Der Veen C, Maurer M, Eichmuller S, Ling G *et al.* (1999) A comprehensive guide for the recognition and classification of distinct stages of hair follicle morphogenesis. *J Invest Dermatol* 113:523–32

Pinnix CC, Herlyn M (2007) The many faces of Notch signaling in skin-derived cells. *Pigment Cell Res* 20:458–65

Roy M, Pear WS, Aster JC (2007) The multifaceted role of Notch in cancer. *Curr Opin Genet Dev* 17:52–9

Schouwey K, Delmas V, Larue L, Zimber-Strobl U, Strobl LJ, Radtke F *et al.* (2007) Notch1 and Notch2 receptors influence progressive hair graying in a dose-dependent manner. *Dev Dyn* 236:282–9

Slominski A, Paus R (1993) Melanogenesis is coupled to murine anagen: toward new concepts for the role of melanocytes and the regulation of melanogenesis in hair growth. *J Invest Dermatol* 101:90S–7S

Takemoto Y, Keighren M, Jackson IJ, Yamamoto H (2006) Genomic localization of a Dct-LacZ transgene locus: a simple assay for transgene status. *Pigment Cell Res* 19:644–5

Tiede S, Kloepper JE, Bodo E, Tiwari S, Kruse C, Paus R (2007) Hair follicle stem cells: walking the maze. *Eur J Cell Biol* 86:355–76

Vasyutina E, Lenhard DC, Wende H, Erdmann B, Epstein JA, Birchmeier C (2007) RBP-J (Rbpsuh) is essential to maintain muscle progenitor cells and to generate satellite cells. *Proc Natl Acad Sci USA* 104: 4443–8

Yoon K, Gaiano N (2005) Notch signaling in the mammalian central nervous system: insights from mouse mutants. *Nat Neurosci* 8:709–15